Seismic risk assessment of frame structures with stochastic properties

M. Fragiadakis
University of Cyprus, Cyprus

G. Stefanou
National Technical University of Athens, Greece

15 WCEE
LISBOA 2012

SUMMARY:
A novel modelling approach is presented for the seismic risk assessment of frames with stochastic system properties. The proposed modelling is based on a mixed fiber beam-column finite element (FE), whose kinematics follow the natural mode method. The FE formulation allows consistently varying the uncertain system properties, which are described by homogeneous non-Gaussian translation stochastic fields. As uncertain parameters we consider the stiffness and the strength of the frame beams and columns. Aleatory uncertainty in the loading can be taken into account using both natural and synthetic ground motion records. The proposed method is used to compute the nonlinear stochastic response and reliability of a three-storey steel moment-resisting frame using Monte Carlo simulation. Useful conclusions are provided regarding the effect of the spectral characteristics of the stochastic fields on the response variability and reliability of the structure.

Keywords: Risk assessment, non-Gaussian stochastic fields, earthquake loading, fiber approach.

1. INTRODUCTION

The efficient prediction of the nonlinear dynamic response of structures with uncertain system properties poses even today a major challenge in the field of computational stochastic mechanics, as opposed to the linear case. This can be explained by the fact that most of the methods developed for the analysis of linear systems are inefficient or inapplicable to the nonlinear case. For example, the analysis of uncertain nonlinear systems is generally not feasible using frequency domain analysis techniques (Iwan & Huang 1996). The existing methods for response statistics calculation in this case are mostly based on simulation (Schuëller & Pradlwarter 1999, Muscolino *et al.* 2003), or on the perturbation approach (Liu *et al.* 1986). Applications of the response surface method have also been proposed (Huh & Haldar 2001), while studies can be found on the statistical equivalent linearization (EQL) method for the response variability and reliability estimation of discrete nonlinear systems (Proppe *et al.* 2003). Alternatively, a probability density evolution method (PDEM) has been developed for this purpose (Li & Chen 2006).We assume that the uncertain system properties can be described by non-Gaussian translation processes. It is worth noting that this theory is able to deliver accurate results for the case of linear and nonlinear dynamic systems assuming stationary output but can be easily extended to a special class of non-stationary, non-ergodic output (Field & Grigoriu 2009).

In order to investigate real-life structural problems subjected to seismic loading, a novel approach, combining Monte Carlo simulation and nonlinear response history analysis with the stochastic field theory has been recently introduced (Stefanou & Fragiadakis 2009). The proposed methodology is used here to assess the response variability and reliability of a benchmark three-storey steel moment-resisting frame. The structure is modelled with a mixed fiber-based, beam-column element, whose kinematics is based on the natural mode method. The adopted formulation leads to the reduction of the cost required for the computation of the element stiffness matrix, while increased accuracy compared to traditional displacement-based elements is achieved (Papachristidis *et al.* 2010). The uncertain parameters are the Young modulus and the yield stress, both described by homogeneous non-Gaussian translation stochastic fields (Grigoriu 1998). Under the assumption of a pre-specified power spectral density function of the stochastic fields describing the two uncertain parameters, the response variability and reliability of the frame is calculated using Monte Carlo simulation. Finally, a parametric investigation is carried out providing useful conclusions regarding the influence of the spectral characteristics of the stochastic fields on the response variability

2. GROUND MOTION RECORDS

2.1. Set of natural ground motions

As seismic input we use both natural and synthetic ground motions. The set of natural records consists of 15 records, divided to three subsets of increasing hazard. i.e. low, medium and high. The records chosen differ in terms of amplitude, frequency content, duration, etc and therefore this variability is expected to be transferred to the statistics of the analysis, producing significant record-to-record variability.

2.2. Stochastic representation of ground motions

Apart from natural records, it is also possible to generate synthetic ground motions using a simple process that has been proposed by Mavroeidis & Papageorgiou (2003). This approach, allows to combine independent models that describe the low-frequency (long period) component, with models that describe the high–frequency component of an acceleration timehistory. A successful application of this approach is given in Taflanidis *et al.* (2008). The generation of the high-frequency component is based on the stochastic (or engineering) approach discussed in detail in Boore (2003). Based on a given magnitude-distance scenario (M_w-R) and depending on a number of site characteristics, the stochastic approach produces synthetic ground motions. The detailed description of the stochastic approach is beyond the scope of this paper. The long-period component is based on the model of Mavroeidis & Papageorgiou (2003). This model is based on an expression that has been calibrated using actual near-field ground motions from all-over the world. Therefore, the velocity pulse of a record is given by the expression:

$$
\begin{aligned}
& v(t) = 0.5A_p\left[1+\cos\left(\frac{2\pi f_p}{\gamma_p}(t-t_0)\right)\right]\cos\left[2\pi f_p(t-t_0)+v_p\right], \\
& t \in \left[t_0 - \frac{\gamma_p}{2f_p}, t_0 + \frac{\gamma_p}{2f_p}\right]
\end{aligned}
\tag{2.1}
$$

where A_p, f_p, v_p, γ_p and t_0 describe the signal amplitude, prevailing frequency, phase angle, oscillatory character (i.e., number of half cycles) and time shift to specify the epoch of the envelope's peak, respectively. All parameters of Eqn. (2.1) have a clear and unambiguous meaning. Depending on the magnitude-distance scenario (M_w-R) examined, the pulse amplitude A_p and frequency f_p are given by the expressions of Rupakhety *et al.* (2011). Thus, the mean A_p value is obtained as:

$$
\log(A_p) = -5.17 + 1.98\cdot M_w - 0.14\cdot M_w^2 - 0.10\cdot\log\left(D^2+0.562\right) \tag{2.2}
$$

where M_w=min(M_w, M_{sat}) and M_{sat}=7.0. Similarly, the mean pulse frequency f_p is:

$$
\log(1/f_p) = -2.87 + 0.47\cdot M_w \tag{2.3}
$$

Eqns (2.2) and (2.3) use base 10 logarithms and the standard deviation of the logarithms is 0.16 and 0.18, respectively.

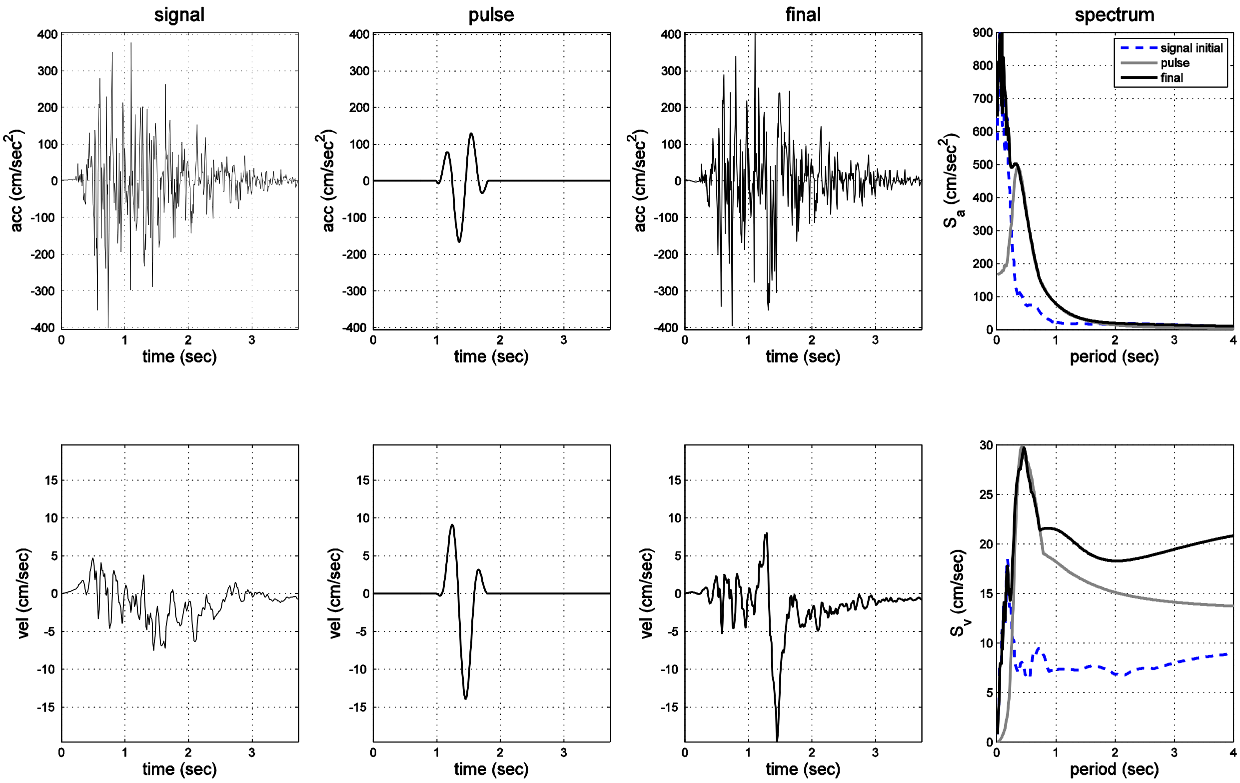

Figure 2.1. Generation of synthetic ground motion records.

The low and high frequency components are combined through the following steps:

1. Sample the moment magnitude M_w and distance R. Assume that the logarithms follow a normal distribution, with mean values provided by Eqn. (2.2) and (2.3) and standard deviation given by Rupakhety *et al.* (2011).
2. Apply the stochastic method to generate an acceleration timehistory to use as the high-frequency component.
3. Generate a velocity pulse using Eqn. (2.1). Shift the pulse so that its maximum velocity coincides in time with the maximum of the velocity time history of the high-frequency record of Step 2.
4. Calculate the Fourier transform of both high and low frequency time histories.
5. Subtract the Fourier amplitude of the pulse from that of the ground motion.
6. Construct a synthetic acceleration time history so that its Fourier amplitude is that of Step 5 and its phase is that of the high-frequency record of Step 2.
7. The final synthetic record is obtained by adding the pulse time history and the time history of Step 6.

The procedure is shown schematically in Figure 2.1. The last column shows the acceleration and velocity spectra, where the effect of the pulse on the spectrum of the outcome timehistory is evident.

3. FINITE ELEMENT FORMULATION

3.1. Force-Based Formulation of the Beam-Column Element

Inelastic analysis of frame structures can be performed either with a lumped or with a distributed plasticity formulation. Distributed plasticity elements are considered more accurate and, in general, are distinguished to displacement-based and to force-based elements. The latter approach, also known as flexibility formulation, has a number of distinct features over the former, especially if it is adopted in the framework of a mixed beam-column formulation (Spacone *et al.* 1996). The force-based formulation requires a single beam-column element per member to simulate its material nonlinear response, since it uses force interpolation functions. Consequently, the element equilibrium is always satisfied, while the compatibility of deformations is satisfied by integrating the section deformations to obtain the element deformations and the nodal displacements. In order to numerically calculate the stiffness matrix, a number of sections along the beam-column element are chosen, while every section is divided to a number of monitoring sections, known as fibers. Fibers are simply integration points of a low order quadrature at the section level and are used to evaluate the section stiffness as follows:

$$\mathbf{D}_{\mathrm{sec}} = \mathbf{k}_{\mathrm{sec}} \mathbf{d}_{\mathrm{sec}} \Leftrightarrow \mathbf{D}_{\mathrm{sec}} = \left(\int_A \frac{\partial \sigma}{\partial \varepsilon} \begin{bmatrix} 1 & -y \\ -y & y^2 \end{bmatrix} dA \right) \mathbf{d}_{\mathrm{sec}} \tag{3.1}$$

where y is the distance of a fiber from the neutral axis, $\mathbf{D}_{\mathrm{sec}}$ are the section forces and $\mathbf{d}_{\mathrm{sec}}=[\varepsilon_{\mathrm{x}}, \kappa]^{\mathrm{T}}$ is the vector of section deformations that consists of the axial strain ε_{x} and the curvature κ. If the response is linear elastic, the diagonal terms of the section stiffness matrix become equal to EA and EI, respectively, while the off-diagonal terms are zero. If the section flexibility matrix is $\mathbf{f}_{\mathrm{sec}} = \mathbf{k}_{\mathrm{sec}}^{-1}$, the element flexibility matrix $\mathbf{F}=\mathbf{K}^{-1}$ is obtained as follows:

$$\mathbf{F} = \mathbf{K}^{-1} = \int_{-1}^{1} \mathbf{b}^T \mathbf{k}_{\mathrm{sec}}^{-1} \mathbf{b}\, d\xi = \int_{-1}^{1} \mathbf{b}^T \mathbf{f}_{\mathrm{sec}} \mathbf{b}\, d\xi = \sum_{i=1}^{NP} w_i \mathbf{b}^T(\xi_i) \mathbf{f}_{\mathrm{sec}}(\xi_i) \mathbf{b}(\xi_i) \tag{3.2}$$

The above equation implies that numerical integration is required in order to obtain the element flexibility matrix, where NP is the number of integration points along the element. In force-based elements, the Gauss-Lobatto quadrature is preferred because it considers as sections of integration the beam ends where the bending moment is maximum, provided that no other element loads are present. This integration scheme requires at least three integration sections, while typically four to six sections are chosen.

The kinematics of the element used in this study follow the principles of the natural mode method proposed in Argyris *et al.* (1988). According to the natural mode method, the displacement field can be decomposed into three rigid body modes $\boldsymbol{\rho}_0$ and three straining modes $\boldsymbol{\rho}_{\mathrm{N}}$ shown in Fig. 3.1. In a flexibility-based element, the calculation of the natural element forces is performed iteratively for every element. The first step of the iterative procedure is to determine the vector of the natural forces. Then using force interpolation functions, the section forces are obtained and subsequently they are corrected according to the constitutive law. The section deformations are obtained from the corrected forces using Eqn. (3.1) and are then integrated according to:

$$\boldsymbol{\rho}_{\mathrm{N}} = \int_{-1}^{1} \mathbf{b}^T(\xi) \mathbf{d}_{\mathrm{sec}}\, d\xi \tag{3.3}$$

in order to obtain the residual natural modes. $\mathbf{b}$ is the interpolation matrix, which is a function of the natural coordinate $\xi \in [-1,1]$ along the element. The iterative process in the element level is terminated when a convergence criterion is satisfied.

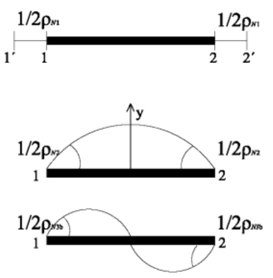

ρ_{N1} extension

ρ_{N2} symmetric bending

ρ_{N3} antisymmetric bending

Figure 3.1. Natural straining modes.

3.2. Stochastic Stiffness Matrix

In the context of stochastic finite element analysis, the uncertain system properties are usually represented by stochastic fields (Stefanou & Papadrakakis 2004). The statistical properties of these fields are based either on experimental measurements or on an assumed variation. In this work, the Young modulus E and the yield stress σ_y of the structure are assumed to be described by two uncorrelated 1D-1V homogeneous non-Gaussian stochastic fields:

$$E(x) = E_0\left[1 + f_1(x)\right] \tag{3.4}$$

$$\sigma_y(x) = \sigma_{y0}\left[1 + f_2(x)\right] \tag{3.5}$$

where E_0 is the mean value of the Young modulus, σ_{y0} is the mean value of the yield stress of the material and $f_1(x)$, $f_2(x)$ are two zero-mean non-Gaussian homogeneous stochastic fields corresponding to the variability of the Young modulus and the yield stress, respectively. Since the entries of the element flexibility matrix are nonlinear functions of the uncertain material properties, it is not possible to establish a closed form expression for the stochastic flexibility matrix. However, an analytical expression of the section stiffness matrix with stochastic material properties can be derived, see Stefanou & Fragiadakis (2009). The stochastic element flexibility matrix of the beam-column element is calculated numerically using its deterministic formulation and the stochastic stiffness.

4. SIMULATION OF NON-GAUSSIAN SYSTEM PROPERTIES

In this paper, a non-Gaussian assumption is made for the distribution of the uncertain parameters of the frame. This choice is in accordance with the fact that several quantities arising in practical engineering problems (e.g. material and geometric properties of structural systems, soil properties, wind loads, waves) are found to exhibit non-Gaussian probabilistic characteristics. In addition, the non-Gaussian assumption permits to efficiently treat the case of large input variability without violating the physical constraints of the material properties.

A number of studies in the literature have been focused on producing a realistic definition of a non-Gaussian sample function from a simple transformation of an underlying Gaussian field with known second-order statistics. Thus, if $g(x)$ is a homogeneous zero-mean Gaussian field with unit variance and spectral density function (SDF) $S_{gg}(\kappa)$, a homogeneous non-Gaussian stochastic field $f(x)$ with power spectrum $S_{ff}^{T}(\kappa)$ is defined as:

$$f(x) = F^{-1} \cdot \Phi\left[g(x)\right] \tag{4.1}$$

where Φ is the standard Gaussian cumulative distribution function and F is the non-Gaussian marginal cumulative distribution function (CDF) of $f(x)$. The transform $F^{-1} \cdot \Phi$ is a memory-less translation since the value of $f(x)$ at an arbitrary point x depends on the value of $g(x)$ at the same point only and the resulting non-Gaussian field is called a translation field (Grigoriu 1998). Translation fields have a number of useful properties such as the analytical calculation of crossing rates and extreme value distributions.

In the present work, Eqn. (4.1) is used for the generation of non-Gaussian translation sample functions representing the uncertain system properties. Sample functions of the underlying Gaussian field $g(x)$ are generated using the spectral representation method (Shinozuka & Dedoatis 1991). In order to investigate the effect of correlation structure on the results, two types of SDF of $g(x)$ with spectral power concentrated at zero frequency and also shifted away from it, are used in the numerical example:

$$S_{gg}(\kappa) = \frac{\sigma_g^2 b}{2\sqrt{\pi}} \exp\left(-\frac{b^2\kappa^2}{4}\right) \tag{4.2}$$

$$S_{gg}(\kappa) = \frac{1}{4}\sigma_g^2 b^3 \kappa^2 \exp\left(-b|\kappa|\right) \tag{4.3}$$

where σ_g is the standard deviation of $g(x)$ and b denotes the parameter that influences the shape of the spectrum and is proportional to the correlation length of the stochastic field along the x-axis. In general, the SDF of the translation field obtained from Eqn. (4.1) will be different from $S_{gg}(\kappa)$. Using the procedure described in this section, a large number of non-Gaussian sample functions are produced and used in MCS to compute the response variability and reliability of the frame.

5. NUMERICAL EXAMPLE

The three-storey steel moment-resisting frame shown in Fig. 5.1 is used for a numerical implementation of the methodology described above. The frame has been designed for a Los Angeles site, following the 1997 NEHRP (National Earthquake Hazard Reduction Program). The dynamic response of the building is dominated by the fundamental mode which has a period value equal to T_1=1.02 sec when the mean value of the modulus of elasticity is used. All response history analyses were performed using a force-based, beam-column fiber element with five integration sections implemented on a general purpose finite element program (Taylor 2000). Geometric nonlinearities were not considered in the analysis. Rayleigh damping is used to obtain a damping ratio of 2% for the first and the fourth mode. The material law is considered to be bilinear with pure kinematic hardening, where the properties of each integration section differ according to the stochastic fields of Eqn. (3.4) and (3.5). The frame section properties are given in Table 5.1. The gravity loading applied is 32.22kN/m for the first two stories and 28.76kN/m for the top storey. These values are used also to obtain the nodal masses resulting to a lumped mass matrix. The results shown here have been obtained using the ground motions of section 2.1.

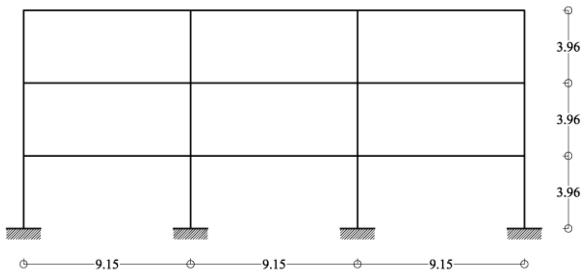

Figure 5.1. The three-storey LA3 steel frame.

The spatial variability in Young modulus and yield stress of the frame is described by two uncorrelated 1D-1V homogeneous non-Gaussian translation stochastic fields with zero mean and coefficient of variation (COV) equal to 0.10. A slightly skewed shifted lognormal distribution defined in the range [-1,+∞] is assumed for the two stochastic fields. The skewness of the lognormal distribution is equal to 0.30. E and σ_y are simultaneously varying in all the cases examined. The representative response quantity whose statistics are monitored is the maximum interstorey drift, which for brevity will be simply referred as drift and denoted as θ_{max}. This parameter is a well-known engineering demand parameter (EDP) that captures the seismic demand and its distributions along the height of the structure. The response statistics have been calculated using 1000 Monte Carlo simulations.

The sensitivity of θ_{max} with respect to the scale of correlation of the stochastic fields, quantified with the aid of the correlation length parameter b of the underlying Gaussian field, is examined for the ground motions of the three sets. For this purpose, several sets of sample functions of E and σ_y are generated using Eqn. (4.1) each for a different value of parameter b. Six representative values of b varying from weak to strong correlation are considered (b = 0.2, 1.0, 2.0, 10, 20 and 100).

Table 5.1. The section properties of the frame.

Storey	Beams	Columns	
		Exterior	Interior
1	W 30×118	W 14×257	W 14×311
2	W 30×116	W 14×257	W 14×311
3	W 24×68	W 14×257	W 14×311

The dynamic response of the frame is highly non-stationary as it can be seen in Fig. 5.2 where the evolution with time of the mean and the COV of θ_{max} are depicted for two correlation length values and for a record of medium intensity. An important observation can be made regarding the variability of θ_{max}. In contrast to the static case where the displacement variability shows always the same trend, starting from small values for small correlation lengths corresponding to white noise stochastic fields up to large values for large correlation lengths (Stefanou & Papadrakakis 2004), the COV of θ_{max} varies significantly not only with the correlation length b but also in different ways among the records of the same intensity level (Fig. 5.3). In some cases, the effect of b becomes negligible and then the record-to-record variability is predominant (e.g. records 1/1, 5/1 and 3/3). In addition, a large magnification of uncertainty is observed in some cases, which is more pronounced for records 1/1, 4/1, 4/2 and 5/2, where the response COV tends to values that are 1.4-1.8 times greater than the corresponding input COV(=0.1). When stochastic earthquake loading is considered in addition to uncertain system properties, the magnification of uncertainty becomes even more pronounced. In contrast, the mean value of drift, although presenting an important record-to-record variability, is practically not affected by the correlation length parameter b (not shown).

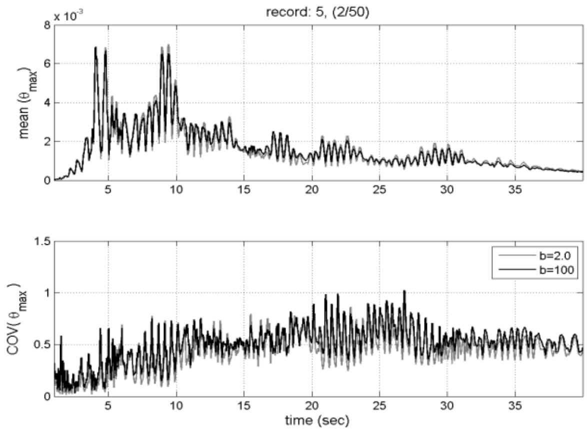

Figure 5.2. Time histories of mean, COV(θ_{max}) – lognormal distribution of E, σ_y for a single record. The time histories are shown for b=2.0 and 100.

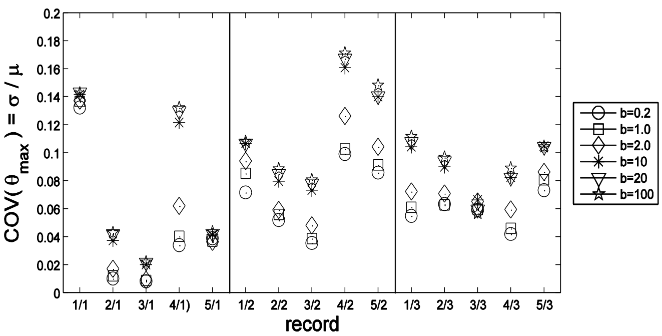

Figure 5.3. COV(θ_{max}) for different values of correlation length parameter b.

Using the results obtained in this section, the reliability of the frame can finally be calculated. Fig. 5.4 shows the CDF of θ_{max} (for a single record) for b=1and 100. If the reliability of the frame is defined as the maximum interstorey drift not exceeding a threshold e.g. 6.5×10^{-3}, the reliability can be obtained from Fig. 5.4 for both cases of b as 0.915 and 0.555, respectively. It is worth noting that the reliability is substantially smaller in the second case. Fig. 5.5 shows the probability density function (PDF) of θ_{max} for the same two values of b, computed using the kernel density estimation method (Bowman & Azzalini 1997). Simultaneously shown are the normal and lognormal distributions with a mean and standard deviation identical to those of the computed PDF, and the extreme value distribution with the same mean as that of the computed PDF. It can be observed that these widely adopted probability distributions are quite different from the real PDF of the response, which clearly has a bimodal form especially in the case of small correlation length.

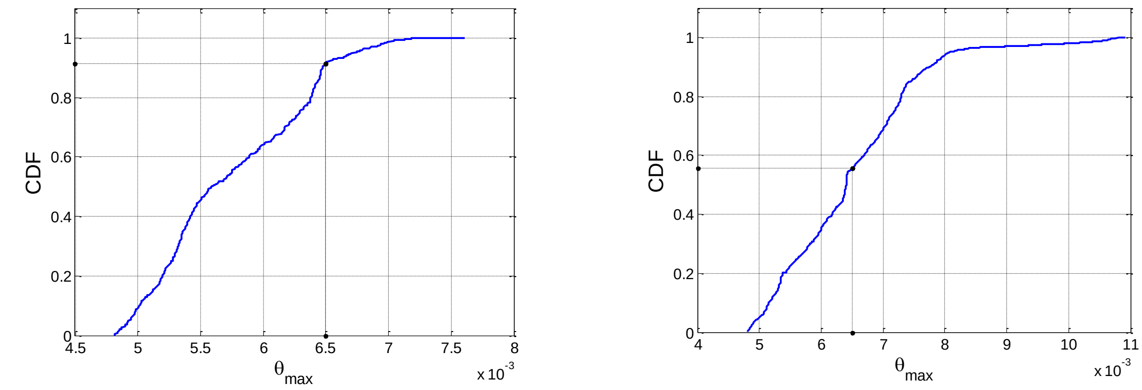

(a) (b)

Figure 5.4. CDF of θ_{max} of record 4/2 for correlation length parameter: (a) b=1 and (b) b=100.

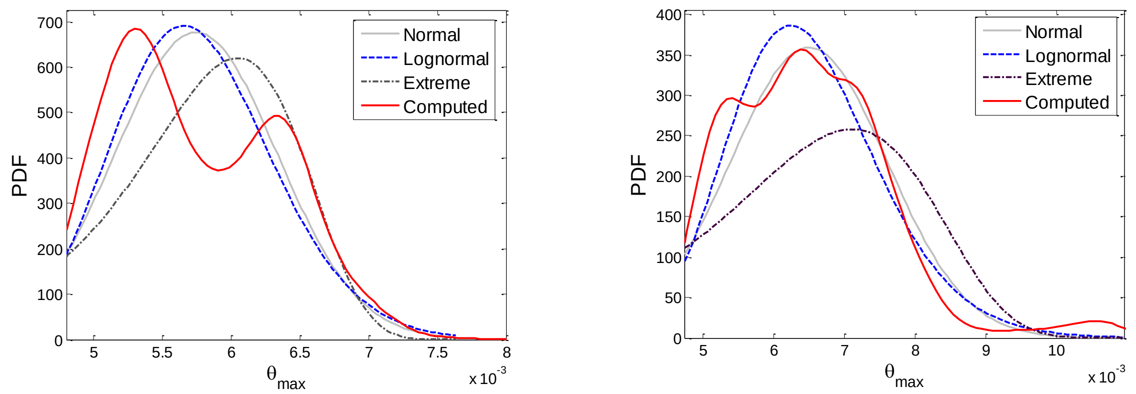

(a) (b)

Figure 5.5. PDF of θ_{max} of record 4/2 for correlation length parameter: (a) b=1 and (b) b=100.

5. CONCLUSIONS

A stochastic response history and reliability analysis of a steel frame having uncertain non-Gaussian material parameters and subjected to seismic loading has been performed. The frame is modeled with a mixed fiber-based, beam-column element, whose kinematics are based on the natural mode method. The adopted formulation provides increased accuracy compared to traditional displacement-based elements and offers significant computational advantages for the analysis of systems with stochastic properties. Two uncorrelated 1D-1V homogeneous non-Gaussian translation stochastic fields with prescribed marginal CDF and SDF have been used for the description of the random spatial fluctuation of the material properties. The variability of the maximum interstorey drift θ_{max} and the reliability of the frame have been computed using MCS.

A parametric investigation revealed the significant influence of the scale of correlation of the stochastic fields (quantified via the correlation length parameter *b*) and of the different seismic records on the response variability: the COV and skewness of θ_{max} have been found to vary quantitatively with *b* and in many different ways between the records of the same intensity level. Finally, a large magnification of uncertainty has been observed in some cases, leading to response COV values that were 1.4-1.8 times greater than those of the input COV. This magnification of uncertainty can be even more pronounced when stochastic earthquake loading is considered in addition to uncertain system properties. These observations underline the importance of a realistic uncertainty quantification and propagation in nonlinear dynamic analysis of engineering systems.

REFERENCES

Argyris, J., Tenek, L., Mattsson, A. (1988). BEC: A 2-node fast converging shear-deformable isotropic and composite beam element based on 6 rigid-body and 6 straining modes. *Comput Methods Appl Mech Engrg*,**152**, 281-336.

Boore, D.M. (2003). Simulation of Ground Motion Using the Stochastic Method. *Pure and Applied Geophysics*, **160**, 653-676.

Bowman, AW, Azzalini, A. (1997). Applied Smoothing Techniques for Data Analysis, Oxford University Press, UK.

Field, R.V. Jr., Grigoriu, M. (2009). Reliability of dynamic systems under limited information. *Probab. Engrg. Mech*. **24**, 16-26.

Grigoriu, M. (1998). Simulation of stationary non-Gaussian translation processes. *J Engrg Mech (ASCE)*, **124**, 121-126.

Huh, J., Haldar, A. (2001). Stochastic finite element-based seismic risk of nonlinear structures. *J Struct Engrg (ASCE)*, **127**, 323-329.

Iwan WD, Huang CT (1996) On the dynamic response of nonlinear systems with parameter uncertainties. *Internat J Non-Linear Mech*,**31**, 631-645.

Lagaros, ND, Fragiadakis, M. (2007). Fragility assessment of steel frames using neural networks. *Earthq Spectra*, **23**,735-752.

Li, J., Chen, J.B. (2006). The probability density evolution method for dynamic response analysis of nonlinear stochastic structures. *Int J Numer Methods Engrg* **65**, 882-903.

Liu, W.K., Belytschko, T., Mani, A. (1986). Probability finite elements for nonlinear structural dynamics. *Comput. Methods Appl. Mech. Engrg.*, **56**, 61-81.

Mavroeidis, G.P., Papageorgiou, A.S. (2003). A mathematical representation of near-fault ground motions, *Bulletin of Seismological Society of America*, **93:3**, 1099-1131.

Muscolino G, Ricciardi G, Cacciola P (2003) Monte Carlo simulation in the stochastic analysis of nonlinear systems under external stationary Poisson white noise input. *Internat J Non-Linear Mech*,**38**, 1269-1283.

Papachristidis, A., Fragiadakis, M., Papadrakakis, M. (2010). A high performance shear-deformable fiber beam-column element for inelastic analysis, *Computational Mechanics*, **45**, 553-572.

Proppe, C., Pradlwarter, H.J., Schuëller, G.I. (2003). Equivalent linearization and Monte Carlo simulation in stochastic dynamics. *Probab Engrg Mech*, **18**, 1-15.

Rupakhety, E. Sigurdsson, S.U., Papageorgiou, A.S., Sigbjörnsson, R. (2011). Quantification of ground-motion parameters and response spectra in the near-fault region, *Bull. Earthquake Eng.*, **9**, 893-930.

Schuëller, G.I., Pradlwarter, H.J. (1999). On the stochastic response of nonlinear FE models. *Arch. Appl. Mech.*, **69**, 765-784.

Shinozuka, M, Deodatis, G. (1991). Simulation of stochastic processes by spectral representation, *Appl Mech Rev (ASME)*, **44**, 191-203.

Spacone, E., Filippou, F.C., Taucer, F.F. (1996). Fiber beam-column model for non-linear analysis of R/C frames: Part I. Formulation. *Earthq Eng Struct Dyn*,**25**, 711-725.

Stefanou, G., Fragiadakis, M. (2009). Nonlinear dynamic analysis of frames with stochastic non-Gaussian material properties. *Engineering Structures,* **31**, 1841-1850.

Stefanou, G., Papadrakakis, M. (2004). Stochastic finite element analysis of shells with combined random material and geometric properties, *Comput Methods Appl Mech Engrg*, **193**,139-160.

Taflanidis, A.A., Scruggs, J.T., Beck, J.L. (2008). Probabilistically robust nonlinear design of control systems for base-isolatated structures, *Journal of Structural Contol and Health Monitoring*, **15**, 697-719.

Taylor, R.L. (2000). FEAP: A Finite Element Analysis Program, *User Manual, Version 7.3., Department of Civil and Environmental Engineering,* University of California at Berkeley, Berkeley, California.